SCIENCE CHINA
Information Sciences

• RESEARCH PAPER •

July 2018, Vol. 61 070206:1–070206:13
https://doi.org/10.1007/s11432-017-9339-7

Special Focus on Learning and Real-time Optimization of Automotive Powertrain Systems

Yaw stability control for a rear double-driven electric vehicle using LPV-H_∞ methods

Yonathan WEISS[1], Liron I. ALLERHAND[2] & Shai AROGETI[1*]

[1]*Department of Mechanical Engineering, Ben-Gurion University of the Negev, Beer-Sheva* 8410501*, Israel;*
[2]*BioCatch, Tel-Aviv* 6744332*, Israel*

Received 14 November 2017/Accepted 29 December 2017/Published online 6 June 2018

Abstract This paper presents a new yaw stability controller for a rear double-driven electric vehicle. A linear parameter varying (LPV) model of the vehicle is formulated using longitudinal speed measurement and tire cornering stiffness estimation. The LPV model is then utilized to design a gain-scheduled H_∞ controller with guaranteed stability. Results from simulations, performed with CarSim, show that the new controller improves the vehicle performance and handling even in extreme maneuvers and that it is robust to model parameter uncertainties.

Keywords yaw stability control, electric vehicle, torque vectoring, H_∞ control, gain-scheduling

Citation Weiss Y, Allerhand L I, Arogeti S. Yaw stability control for a rear double-driven electric vehicle using LPV-H_∞ methods. Sci China Inf Sci, 2018, 61(7): 070206, https://doi.org/10.1007/s11432-017-9339-7

1 Introduction

In recent years, due to growing awareness of environmental issues and the global aspiration to reduce the emission of pollutants, the development of electric powered passenger vehicles has accelerated. Beyond the environmental benefits of electric vehicles, which do not emit pollutants at all, this type of vehicles allows separate propulsion of each driving wheel by an electric motor connected to it directly. This type of direct propulsion of each driving wheel is not only space economic and allows good energy management, but also constitutes an advantage in the field of stability control. It enables driving torque based stability control instead of the traditional one, based on brake-torque. Electric motors are highly responsive and their torque output can be controlled accurately. These qualities can have a great impact on the transient and steady state handling response of the vehicle. In addition, torque vectoring (TV)[1)] applied through individual wheel propulsion does not suffer from the mechanical limitations of active differentials, and therefore is more efficient [2].

Yaw stability control (YSC) systems are active safety systems designed to reduce accidents occurrence due to directional instability. As of 2012, all manufacturers in the USA are obligated to incorporate such systems in their vehicles [3]. It is therefore not surprising that the field of YSC systems has received much academic interest in the last years. The majority of YSC systems share a hierarchical structure, comprised of an upper controller and a lower controller. The upper controller receives data from vehicle sensors, such as steering wheel angle, speed and yaw rate, then calculates the required yaw moment in order to

* Corresponding author (email: arogeti@bgu.ac.il)

1) Torque vectoring is defined as applying different torque magnitudes on the driving wheels, thus generating yaw moment [1].

track desired values of yaw rate and sideslip angle. The lower controller operates the actuators; these can be the vehicle brakes, active differential torque transfer or electric motors [4]. Many control methods have been suggested for the design of the upper controller. The simplest controllers were those based on a linearized model, with control methods that include mostly linear quadratic regulator (LQR) [5–9] and H_∞ control [10]. More advanced approach used for dealing with the nonlinearities, inherent in the vehicle dynamics, is the sliding mode control (SMC), either by using linearized model and treat nonlinearities as model uncertainty, as done in [11–13], or by incorporating the nonlinear model directly in the design [14,15]. Fuzzy logic control (FLC) was used in [16,17], introducing a set of logic rules that formulate the control law and thus avoiding the complexity of dealing with nonlinear model. Successive linearization was used by [18] to linearize the model around current state and by [19] to linearize the model around current equilibrium point, both applying model predictive control (MPC) methods. A very popular approach for dealing with nonlinearity is gain-scheduling. The term gain-scheduling generally describes the control of a nonlinear system using several linear controllers, which are interpolated or switched online according to the state of the system [20]. Since the description of vehicle dynamics via linear model is inadequate and designing a controller for nonlinear model is complex, this method is quite popular in the filed of vehicle stability control. Several control methods were used with gains scheduling, including proportional-integral-derivative (PID) [2], LQR [21, 22], H_∞ control [23, 24], energy-to-peak control [25, 26], mixed sensitivity loop shaping [27] and even MPC [28]. The scheduling parameters for the controllers were also diverse and varied between several combinations; longitudinal speed [24–26], longitudinal speed and yaw rate [27], longitudinal speed and steering input [22], longitudinal speed and cornering stiffness [21], tire slip angles and slip ratio [23], longitudinal acceleration along with steering input and friction coefficient [2].

In this study, a new controller is designed based on a linear parameter varying (LPV) model of the vehicle, which depends on the longitudinal speed and cornering stiffness of the tires. External changes, such as steering, excite the system and induce errors in the reference tracking of the system. Our goal is to minimize the induced errors in the lateral velocity and the yaw rate. Since steering is hard to model, we aim to guarantee performance for any steering signal. Mathematically this means that we minimize the induced L_2 norm from the external signals to the objective vector. This design method is referred to as H_∞ control [29]. The novelty of this study is in the successful integration of a cornering stiffness estimator which rely solely on measurements of the vehicle velocities and accelerations. The use of this estimation method allows the controller to be independent of any prior knowledge regarding the tire-road friction coefficient while still being effective in a wide range of driving conditions. The controller itself is unique thanks to the chosen time-varying parameters in the LPV model used in its design. The H_∞ method was also used before to design gain-scheduled controllers. However, the gain-scheduled controllers relied only on varying speed and the cornering stiffness was treated mostly with norm-bounded uncertainty approach (i.e., a robust approach), thus keeping the design very conservative. In contrast with other methods proposed in previous studies, such as LQR and MPC, this gain-scheduled H_∞ controller guarantees closed-loop stability in a wide range of operating conditions, using LPV framework. Such a controller can provide excellent performance while being relatively simple to design and implement.

2 LPV vehicle model

A well-known vehicle model, used for control design and dynamics analysis, is the so-called bicycle model [4,30–32]. This two degrees-of-freedom (2DOF) linear model describes the lateral and yaw motions of the vehicle (see Figure 1), as follows:

$$\dot{x}_p = A_p x_p + B_{p1} w_p + B_{p2} u_p, \tag{1}$$

where

$$x_p = \begin{bmatrix} V_y & \dot{\psi} \end{bmatrix}^{\mathrm{T}}, \quad w_p = \delta, \quad u_p = M_z,$$

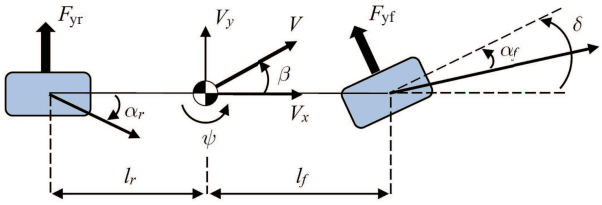

Figure 1 (Color online) 2DOF vehicle model.

$$A_p = \begin{bmatrix} -\dfrac{C_{\alpha f}+C_{\alpha r}}{mV_x} & -\left(V_x + \dfrac{l_f C_{\alpha f} - l_r C_{\alpha r}}{mV_x}\right) \\ -\dfrac{l_f C_{\alpha f} - l_r C_{\alpha r}}{I_{zz} V_x} & -\dfrac{l_f^2 C_{\alpha f} + l_r^2 C_{\alpha r}}{I_{zz} V_x} \end{bmatrix},$$

$$B_{p1} = \begin{bmatrix} \dfrac{C_{\alpha f}}{m} & \dfrac{l_f C_{\alpha f}}{I_{zz}} \end{bmatrix}^{\mathrm{T}}, \quad B_{p2} = \begin{bmatrix} 0 & \dfrac{1}{I_{zz}} \end{bmatrix}^{\mathrm{T}}.$$

The two states, V_y and $\dot{\psi}$, are the lateral velocity of the vehicle and its yaw rate, respectively. The longitudinal velocity, V_x, is considered a constant (in this model) and therefore is not taken as a state. The mass of the vehicle and its yaw moment of inertia are denoted, respectively, by m and I_{zz}. The distances between the vehicle's center of gravity and the axles are l_r, for the rear axle, and l_f, for the front axle. The cornering stiffness of the rear and front tires are $C_{\alpha r}$ and $C_{\alpha f}$, respectively. The steering angle, denoted by δ, is considered as a disturbance input as it is not determined by the control system. The control input of the system is the stabilizing yaw moment, M_z.

2.1 Cornering stiffness estimation

Cornering stiffness of a tire is defined as the slope of the lateral force curve at zero slip angle [33]. When the slip angle of a tire is small, it is proportional to the lateral force

$$F_y = C_\alpha \alpha. \tag{2}$$

Here, α is the slip angle and C_α denotes the cornering stiffness of a tire at nominal conditions, namely, nominal normal load, tire-road friction coefficient, air pressure and others. When the slip angle increases significantly or when there are large deviations from the nominal conditions, the above relation between the lateral force and the slip angle becomes inaccurate. The purpose of cornering stiffness estimation, as presented here, is to update the value of the C_α continuously, such that at each instant the relation in (2) remains accurate regardless of condition and slip angle variations.

In this study, an estimated method presented in [34] and referred to as the direct method, is used. The main idea behind this method is simply taking the differential equations for the lateral velocity and the yaw rate from (1) and rearrange them such that, given the values V_y, $\dot{V}_y$, $\dot{\psi}$, $\ddot{\psi}$ and δ, algebraic solutions for the estimation of $C_{\alpha r}$ and $C_{\alpha f}$ are obtained

$$C_{\alpha r}(t) = \frac{(ml_f\dot{V}_y - ml_f\dot{\psi}V_x - I_{zz}\ddot{\psi})/L}{(l_r\dot{\psi} - V_y)/V_x}, \tag{3}$$

$$C_{\alpha f}(t) = \frac{(ml_r\dot{V}_y + ml_r\dot{\psi}V_x + I_{zz}\ddot{\psi})/L}{(-V_y - l_f\dot{\psi} + V_x\delta)/V_x}, \tag{4}$$

where $L = l_r + l_f$ is the wheel base of the vehicle.

One can easily verify that the expressions in the denominators of (3) and (4) are the same as the ones used to describe the rear and front slip angles, receptively, in the 2DOF linear model [4]. This means that when the slip angles approach zero, due to either, straight driving or transient conditions, the cornering stiffness values will approach infinity. This calls for limitation of the estimation process such that its

values will be used only within certain bounds and discarded outside. Here, the values of the cornering stiffness were bounded as follows:

$$\begin{aligned} 1\cdot 10^4 \text{ N/rad} \leqslant C_{\alpha r} \leqslant 5\cdot 10^5 \text{ N/rad},\\ 1\cdot 10^4 \text{ N/rad} \leqslant C_{\alpha f} \leqslant 5\cdot 10^5 \text{ N/rad}. \end{aligned} \tag{5}$$

Simulations using a full vehicle model showed that the ratio of lateral force to slip angle stays between these values in most scenarios. In addition, relaxations of these constraints showed no significant improvement in the LPV model accuracy.

2.2 Polytopic LPV model

A polytopic LPV vehicle model is now formulated using the stiffness estimates and the measurement of the longitudinal velocity. In general, an LPV system has a state space representation which depends on an exogenous time-varying parameter vector $\theta \in \mathcal{R}^l$, as follows [35]:

$$\begin{aligned} \dot{x} &= A(\theta)x + B_1(\theta)w + B_2(\theta)u,\\ z &= C_1(\theta)x + D_{12}(\theta)u. \end{aligned} \tag{6}$$

The LPV system in (6) is referred to as a polytopic LPV system if it can be represented by a convex combination of LTI systems, namely,

$$\begin{aligned} &\begin{pmatrix} A(\theta) & B_1(\theta) & B_2(\theta)\\ C_1(\theta) & D_{12}(\theta) & * \end{pmatrix} = \sum_{i=1}^{N} \rho_i(\theta) \begin{pmatrix} A^{(i)} & B_1^{(i)} & B_2^{(i)}\\ C_1^{(i)} & D_{12}^{(i)} & * \end{pmatrix},\\ &\sum_{i=1}^{N} \rho_i(\theta) = 1, \ \ \rho_i(\theta) \geqslant 0, \ \ N = 2^l, \end{aligned} \tag{7}$$

where $A^{(i)}$, $B_1^{(i)}$, $B_2^{(i)}$, $C_1^{(i)}$, and $D_{12}^{(i)}$ denote the state-space representation of the system dynamics at the vertices of the polytope. The scheduling parameters ρ_i are functions of the system parameters, which are represented by the vector θ. The vector z is the objective vector (or the controlled output) of the controlled system, it will take part in the representation of the yaw stability control goal.

In order to formulate a polytopic LPV model of the vehicle, the time-varying parameters should appear linearly in the model [36]. Since this is not the case here, four new parameters are defined, which may vary within some known bounds:

$$\begin{aligned} \theta_1(t) &= V_x(t) \in [V_{x\_\min}, V_{x\_\max}],\\ \theta_2(t) &= C_{\alpha f}(t) \in [C_{\alpha f\_\min}, C_{\alpha f\_\max}],\\ \theta_3(t) &= \frac{C_{\alpha f}(t)}{V_x(t)} \in \left[\left(\frac{C_{\alpha f}}{V_x}\right)_{\min}, \left(\frac{C_{\alpha f}}{V_x}\right)_{\max}\right],\\ \theta_4(t) &= \frac{C_{\alpha r}(t)}{V_x(t)} \in \left[\left(\frac{C_{\alpha r}}{V_x}\right)_{\min}, \left(\frac{C_{\alpha r}}{V_x}\right)_{\max}\right]. \end{aligned} \tag{8}$$

For this design, the cornering stiffnesses were allowed to vary between the bounds defined in (5) and the longitudinal velocity was limited to vary between 70 and 140 km/h. The longitudinal velocity limitation takes into account the velocity range in which a driver is likely to drive and the velocities at which the YSC system is needed. Using the new parameters defined above, the 2DOF LPV model can be reformulated as follows:

$$\dot{x}_p = A_p(\theta)\, x_p + B_{p1}(\theta)\, w_p + B_{p2} u_p, \tag{9}$$

where

$$x_p = \left[V_y \ \dot{\psi}\right]^{\mathrm{T}}, \ \ w_p = \delta, \ \ u_p = M_z,$$

$$A_p(\theta) = \begin{bmatrix} -\dfrac{1}{m}(\theta_3+\theta_4) & -\left(\theta_1+\dfrac{1}{m}(l_f\theta_3 - l_r\theta_4)\right) \\ -\dfrac{1}{I_{zz}}(l_f\theta_3 - l_r\theta_4) & -\dfrac{1}{I_{zz}}\left(l_f^2\theta_3 + l_r^2\theta_4\right) \end{bmatrix},$$

$$B_{p1} = \begin{bmatrix} \dfrac{1}{m}\theta_2 & \dfrac{l_f}{I_{zz}}\theta_2 \end{bmatrix}^{\mathrm{T}}, \quad B_{p2} = \begin{bmatrix} 0 & \dfrac{1}{I_{zz}} \end{bmatrix}^{\mathrm{T}}.$$

3 Control objectives

The control objectives, namely, the desired values for the yaw rate and the lateral velocity are calculated based on the driver's inputs, steering wheel angle and throttle position. As mentioned in the NHTSA's official regulations regarding ESC systems [3], the average driver is used to operate the vehicle in its linear region, therefore his driving skills are adjusted to this kind of vehicle behavior. In order to meet driver's expectations from the vehicle, especially in severe maneuvers, the desired values for the control system are derived based on the 2DOF linear model (bicycle model) analysis. For steady state circular motion the angular velocity equals V/R, therefore the desired yaw rate can be approximated as

$$\dot{\psi}_{\mathrm{ss}} = \frac{V_x}{R}, \tag{10}$$

where $1/R$ is the desired path curvature for a given steering angle, given by

$$\frac{1}{R} = \frac{\delta}{L + K_{\mathrm{us}} V_x^2}, \tag{11}$$

and K_{us}, known as the understeer gradient, is ([30])

$$K_{\mathrm{us}} = \frac{m}{L}\left(\frac{l_r}{C_{\alpha f}} - \frac{l_f}{C_{\alpha r}}\right). \tag{12}$$

The desired value of the lateral velocity can be obtained by solving (1) for its steady state condition

$$V_{y\_\mathrm{ss}} = \frac{1}{R}\left(l_r - \frac{m l_f V_x^2}{L C_{\alpha r}}\right) V_x. \tag{13}$$

Since tracking the values presented in (10) and (13) is not always feasible, or it is not safe due to driving conditions, limitations on these values are introduced. Using lateral force balance, [4] suggests the next upper bound for the yaw rate

$$\dot{\psi}_{\max} = 0.85\frac{\mu g}{V_x}, \tag{14}$$

and regarding the upper bound of the lateral velocity, the following empirical expression is suggested

$$V_{y\_\max} = V_x \cdot \arctan(0.02\mu g). \tag{15}$$

Overall, the desired values for the yaw rate and the lateral velocity can be formulated as

$$\dot{\psi}_d = \begin{cases} \dot{\psi}_{\mathrm{ss}}, & |\dot{\psi}_{\mathrm{ss}}| \leqslant \dot{\psi}_{\max}, \\ \dot{\psi}_{\max} \cdot \mathrm{sgn}(\dot{\psi}_{\mathrm{ss}}), & |\dot{\psi}_{\mathrm{ss}}| > \dot{\psi}_{\max}, \end{cases} \tag{16}$$

$$V_{\mathrm{yd}} = \begin{cases} V_{y\_\mathrm{ss}}, & |V_{y\_\mathrm{ss}}| \leqslant V_{y\_\max}, \\ V_{y\_\max} \cdot \mathrm{sgn}(V_{y\_\mathrm{ss}}), & |V_{y\_\mathrm{ss}}| > V_{y\_\max}. \end{cases} \tag{17}$$

4 Control design

The control system presented here is a hierarchical one (see Figure 2); an upper controller receives data from the vehicle's sensors and driver's commands (throttle and steering input) and calculates the corrective yaw moment required, a lower level controller then determines the torques required from the motors in order to generate the desired yaw moment.

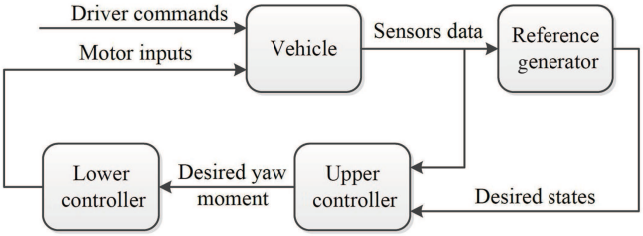

Figure 2 Control system architecture.

4.1 Upper controller

Since the task of the controller is trajectory tracking, a reference model is used. The chosen reference model is a first order filter of the desired state values and its purpose is to generate smooth and differentiable reference signals for the system to follow. Its states follow the first order differential equation

$$\tau\dot{x} + x = r. \tag{18}$$

Thus, the reference model has the following state space representation:

$$\dot{x}_r = A_r x_r + B_{1r} w_r, \tag{19}$$

where

$$x_r = \begin{bmatrix} V_{\mathrm{yr}} & \dot{\psi}_r \end{bmatrix}^{\mathrm{T}}, \quad w_r = \begin{bmatrix} V_{\mathrm{yd}} & \dot{\psi}_d \end{bmatrix},$$
$$A_r = \begin{bmatrix} -\dfrac{1}{\tau_1} & 0 \\ 0 & -\dfrac{1}{\tau_2} \end{bmatrix}, \quad B_{1r} = \begin{bmatrix} \dfrac{1}{\tau_1} & 0 \\ 0 & \dfrac{1}{\tau_2} \end{bmatrix}.$$

One should note that a clear distinction is made here between the desired values and the reference values. The desired values, marked with subscript d, are calculated as shown in Section 3 and may be noisy, not differentiable or even not continuous. The reference values, marked with subscript r, which are filtered versions of the desired values (with time constants of τ_1 and τ_2), are continuous, differentiable, smoother and slower and therefore are easier to track and reduce the risk of aggressive control actions.

The tracking problem is formulated by augmenting the vehicle model to include the reference model states and by defining the output such that it represents a weighted sum of the tracking errors and the control effort. The augmented model is therefore given by

$$\begin{aligned} \dot{x} &= A(\theta)\, x + B_1(\theta)\, w + B_2 u, \\ z &= C_1 x + D_{12} u, \end{aligned} \tag{20}$$

where

$$x = \begin{bmatrix} V_y & \dot{\psi} & V_{\mathrm{yr}} & \dot{\psi}_r \end{bmatrix}^{\mathrm{T}}, \quad w = \begin{bmatrix} \delta & V_{\mathrm{yd}} & \dot{\psi}_d \end{bmatrix}^{\mathrm{T}}, \quad u = M_z,$$
$$A(\theta) = \begin{bmatrix} A_p(\theta) & 0_{2\times 2} \\ 0_{2\times 2} & A_r \end{bmatrix}, \quad B_1(\theta) = \begin{bmatrix} B_{p1}(\theta) & 0_{2\times 2} \\ 0_{2\times 2} & B_{1r} \end{bmatrix}, \quad B_2 = \begin{bmatrix} B_{p2} \\ 0_{2\times 1} \end{bmatrix},$$
$$C_1 = \begin{bmatrix} W_{V_y} & 0 & -W_{V_y} & 0 \\ 0 & W_{\dot{\psi}} & 0 & -W_{\dot{\psi}} \\ 0 & 0 & 0 & 0 \end{bmatrix}, \quad D_{12} = \begin{bmatrix} 0 \\ 0 \\ W_u \end{bmatrix}.$$

Here, W_{V_y} and $W_{\dot{\psi}}$ are the weighting factors for the tracking error of the lateral velocity and the yaw rate, respectively, and W_u is the weighting factor of the control effort magnitude. Writing the output vector z explicitly, we have

$$z = \begin{bmatrix} W_{V_y}(V_y - V_{\mathrm{yr}}) & W_{\dot{\psi}}(\dot{\psi} - \dot{\psi}_r) & W_u M_z \end{bmatrix}^{\mathrm{T}}. \tag{21}$$

We obtained a model whose uncontrolled inputs are the steering angle and the desired state values, its control input is the corrective yaw moment and its output is a weighted sum of the tracking errors of the states and the control effort magnitude. Considering a polytopic state feedback controller of the form

$$u = \sum_{i=1}^{N} \rho_i(\theta) K^{(i)} x, \tag{22}$$

the closed loop of the system in (20) is quadratically stable and its H_∞ norm from w to z is less than a prescribed $\gamma > 0$, if and only if the following LMIs:

$$\begin{aligned} &\begin{bmatrix} A^{(i)}X + XA^{(i)\mathrm{T}} + B_2 Y^{(i)} + Y^{(i)\mathrm{T}} B_2^{\mathrm{T}} & * & * \\ B_1^{(i)\mathrm{T}} & -\gamma^2 I & * \\ C_1 X + D_{12} Y^{(i)} & 0 & -I \end{bmatrix} \leqslant 0, \\ &X > 0 \end{aligned} \tag{23}$$

hold for all system vertices, $i = 1, \ldots, N$. Here, the gain matrices, $K^{(i)} = Y^{(i)} X^{-1}$, are the stabilizing controller gains corresponding to each vertex of the system. The stability of the proposed controller can be shown by substituting the closed loop of the LPV system into the bounded-real lemma; the use of a single X matrix implies quadratic stability [37]. As shown in (22), the gain matrices are interpolated in accordance with the values of the parameter vector θ (i.e., scheduled according to the location of the system inside the polytope). This type of controller is known as gain-scheduled state feedback H_∞ controller.

In the current design, the above LMIs were solved using YALMIP toolbox for MATLAB. The optimal solution was obtained by an iterative process of solving the LMIs with reducing γ until infeasibility is encountered (with this process the minimal value of γ is obtained).

Polytope vertices and scheduling parameters. The vector θ contains four time-varying parameters, each of them is lower and upper bounded (Section 2). Hence, the vehicle augmented LPV model in (20) can be represented by a convex combination of $2^4 = 16$ LTI systems. In accordance with the number of system vertices, the solution to the relevant LMIs yields 16 gain matrices. These matrices are continuously interpolated, using the scheduling variables as shown in (22), to form a single gain matrix to be used in the control law. In this study, the scheduling variables were obtained analytically, as follows:

$$\alpha_j = \frac{\theta_j - \theta_{j_{\min}}}{\theta_{j_{\max}} - \theta_{j_{\min}}}, \quad \beta_{ij} = \begin{cases} \alpha_j, & \text{if } \theta_j^{(i)} = \theta_{\max}, \\ 1 - a_j, & \text{if } \theta_j^{(i)} = \theta_{\min}, \end{cases} \quad \rho_i = \prod_{j=1}^{4} \beta_{ij}. \tag{24}$$

4.2 Lower controller

The lower controller's task is to activate the two rear motors such that the additional yaw moment is applied without loss of total longitudinal force. A torque distribution has to be made such that a difference in longitudinal forces is achieved and, at the same time, the total longitudinal force applied to the vehicle is not reduced, preventing speed reduction. A simple method to achieve this is by increasing torque on one side and reducing torque on the other side, by the same amount, ΔT.

As the additional yaw moment is generated by difference in longitudinal forces at the rear tires, the control moment can be expressed in terms of rear longitudinal forces

$$M_z = \frac{t_r}{2}(F_{\mathrm{xrr}} - F_{\mathrm{xrl}}), \tag{25}$$

where t_r is the rear track width. Rearranging the equation above, the longitudinal force difference needed to produce the desired yaw moment is obtained

$$(F_{\mathrm{xrr}} - F_{\mathrm{xrl}}) = \frac{2M_z}{t_r}. \tag{26}$$

The rear wheels rotational dynamics is given by the following differential equations:

$$J_w\dot{\omega}_{\rm rr} = T_{\rm mrr} - r_{\rm wr}F_{\rm xrr}, \tag{27}$$

$$J_w\dot{\omega}_{\rm rl} = T_{\rm mrl} - r_{\rm wr}F_{\rm xrr}, \tag{28}$$

where J_w is the wheels moment of inertia, $\omega_{\rm rr}$ and $\omega_{\rm rl}$ are the angular velocity of the rear-right and rear-left wheels, respectively, $r_{\rm wr}$ is the effective rolling radius of the rear wheels and $T_{\rm mrr}$ and $T_{\rm mrl}$ are the driving/breaking torques applied by the rear-right and the rear-left motors, respectively. Defining the torque at each motor as a sum of some baseline driving torque (T_d, which is equal for both motors) and an additional torque supplement term

$$T_{\rm mrr} = T_d + \Delta T, \tag{29}$$

$$T_{\rm mrl} = T_d - \Delta T. \tag{30}$$

Substituting the expressions for the motor torques ((29) and (30)) back into the wheels' dynamics in (27) and (28), we have

$$J_w\dot{\omega}_{\rm rr} = T_d + \Delta T - r_{\rm wr}F_{\rm xrr}, \tag{31}$$

$$J_w\dot{\omega}_{\rm rl} = T_d - \Delta T - r_{\rm wr}F_{\rm xrr}. \tag{32}$$

Subtracting (32) from (31)

$$J_w(\dot{\omega}_{\rm rr} - \dot{\omega}_{\rm rl}) = 2\Delta T - r_{\rm wr}(F_{\rm xrr} - F_{\rm xrl}). \tag{33}$$

Substituting from (26) and rearranging, the expression for the desired torque supplement is obtained

$$\Delta T = \frac{r_{\rm wr}}{t_r}M_z + \frac{J_w}{2}(\dot{\omega}_{\rm rr} - \dot{\omega}_{\rm rl}). \tag{34}$$

Now, the desired torque at each motor can be expressed in terms of the control yaw moment M_z

$$T_{\rm mrr} = T_d + \frac{r_{\rm wr}}{t_r}M_z + \frac{J_w}{2}(\dot{\omega}_{\rm rr} - \dot{\omega}_{\rm rl}), \tag{35}$$

$$T_{\rm mrl} = T_d - \frac{r_{\rm wr}}{t_r}M_z - \frac{J_w}{2}(\dot{\omega}_{\rm rr} - \dot{\omega}_{\rm rl}). \tag{36}$$

In the following numerical results, the electric motors' dynamics were simulated as the first order dynamics (see [38]),

$$\frac{L_m}{k_m}\frac{\rm d}{{\rm d}t}(T_m) + \frac{R_m}{k_m}T_m = u_m, \tag{37}$$

where L_m, R_m and k_m are the inductance, resistance and torque constant of the motor, respectively. The input voltage to the motor, u_m, is determined using a proportional integral (PI) controller that regulates the desired torque. Overall the dynamics of the motor torques, from the requested torque to the actual torque, was modeled as a second order linear system. The output torque of each motor was limited, in this study, to 400 Nm, this corresponds to a 80 Nm motor, with a reduction ratio of 1:5.

5 Simulation results

In order to evaluate the performance of the vehicle with the designed gain-scheduled H_∞ (GS-H_∞) controller, simulations were carried out using the CarSim software package. In Subsection 5.1, the proposed controller was tested and compared to a stationary H_∞ controller, namely, a controller, which is based on a linear 2DOF vehicle model with nominal values of cornering stiffness and longitudinal velocity (the nominal velocity was taken as 80 km/h). A robustness test for the gain-scheduled controller is also presented, showing its ability to tolerate model parameter inaccuracies. The model parameters used for the simulations, and for the design of the controller, are presented in Table 1. The vehicle model for validation is generated by the CarSim software package. It is considered a reliable car model, which takes into account the tire-road nonlinear interaction; it was tuned according Table 1. The weights used in the design of the controllers are presented in Table 2.

Table 1 Vehicle model parameters

Parameter	Unit	Value	Parameter	Unit	Value
m	kg	1140	$C_{\alpha r}$	N/rad	135000
I_{zz}	kg·m^2	996	$C_{\alpha f}$	N/rad	150000
l_r	m	1.165	R_m	Ω	0.532
l_f	m	1.165	k_m	Nm/A	21
t_r	m	1.486	L_m	H	0.007
$r_{\rm wr}$	m	0.299	τ_1	s	0.3
J_w	kg·m^2	0.6	τ_1	s	0.3

Table 2 H_∞ controllers' weights

Weight	Stationary	Gain-Scheduled
W_{V_y}	0.5	0.5
$W_{\dot\psi}$	1	1
W_u	$6.2\cdot10^{-7}$	0.135

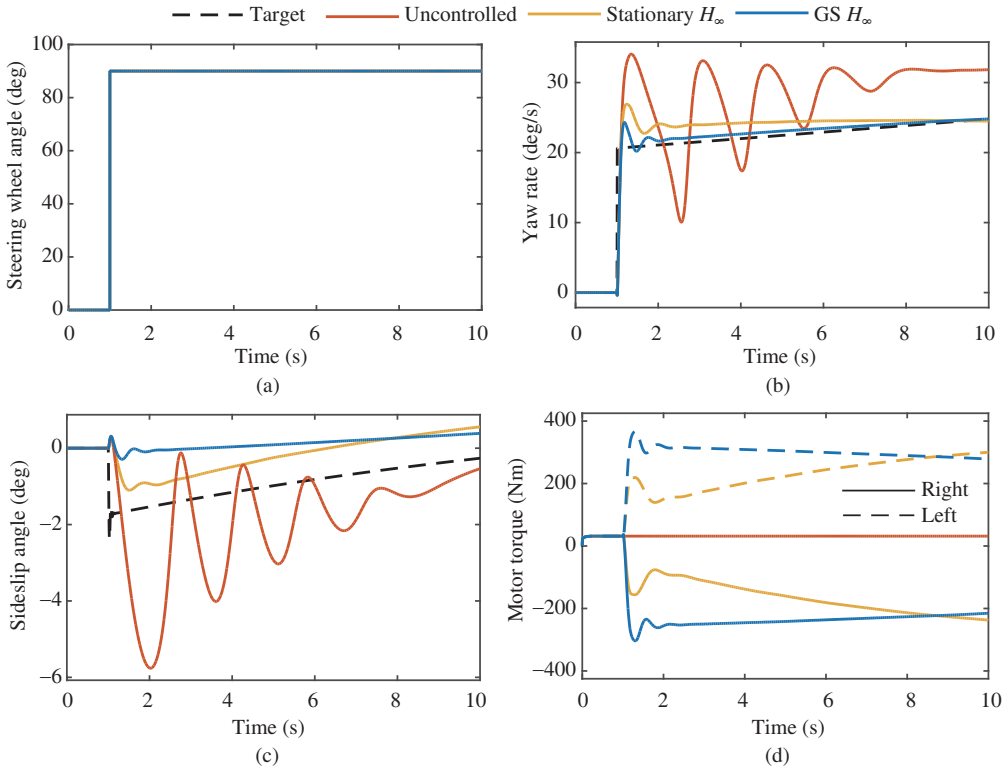

Figure 3 (Color online) Simulation results of step steering test for gain scheduled H_∞ controlled, stationary H_∞ controlled and uncontrolled vehicle. (a) Steering wheel angle; (b) yaw rate; (c) sideslip angle; (d) motor torques.

5.1 Step steering test

In this maneuver, the initial velocity of the vehicle is 75 km/h, and it drives on a dry road ($\mu = 0.85$). After 1 s, in which the motor torques converge to their steady state values (using a speed controller), a steering wheel step input of 90 degrees is applied. In the uncontrolled vehicle the motor torques stay at their steady state value for the entire maneuver, whereas for the controlled vehicle these values are used as baseline torques (from which torque is added or subtracted as needed). The simulation results are presented in Figure 3. It is seen in the results that the proposed GS-H_∞ controller eliminates yaw rate and sideslip angle oscillations, seen in the uncontrolled vehicle, reduces overshoots and presents excellent yaw rate tracking. The yaw rate response of the stationary H_∞ controller is not as good but its sideslip

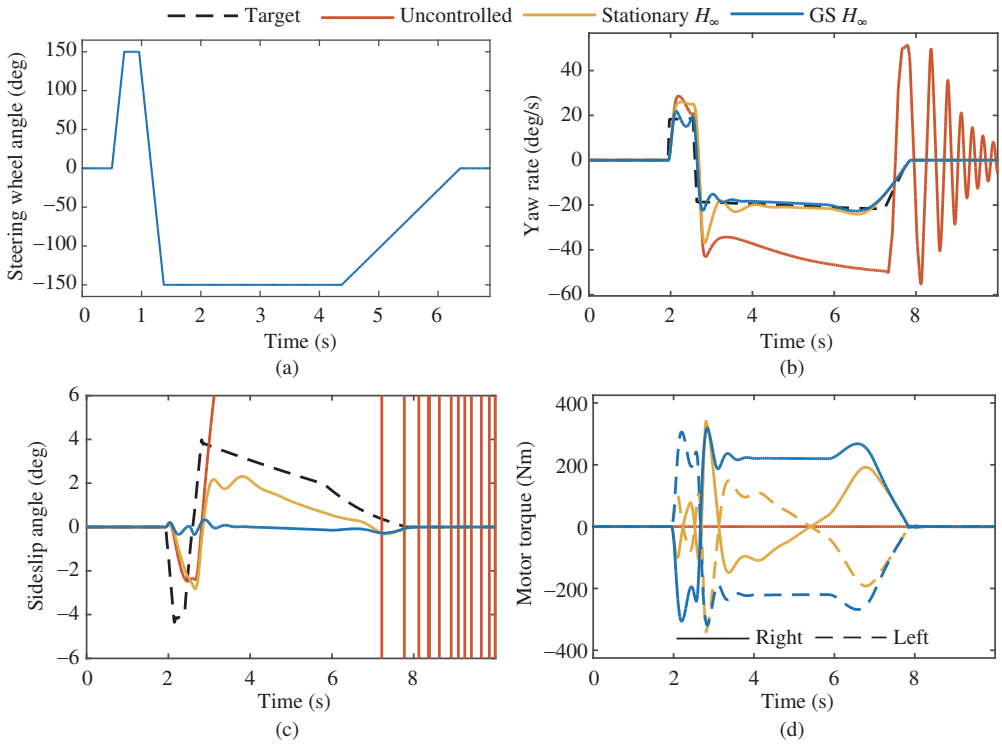

Figure 4 (Color online) Simulation results of fishhook maneuver for gain scheduled H_∞ controlled, stationary H_∞ controlled and uncontrolled vehicle. (a) Steering wheel angle; (b) yaw rate; (c) sideslip angle; (d) motor torques.

angle response is slightly better. It should be mentioned that precise tracking of the sideslip angle is less significant, as long as its values remain small (in fact, in many other yaw controllers suggested in the literature, the desired sideslip angle was taken as zero).

5.2 Fishhook maneuver

In this maneuver, the steering input approximates a driver's panic reaction when trying to regain lane position [39]. The vehicle is driving on a dry road ($\mu = 0.85$) at an initial speed of 82 km/h with no throttle input; the steering input initiates when the speed drops to 80 km/h. The steering input (see Figure 4(a)) begins with a ramp steer of 720 deg/s until it reaches a magnitude of 150 deg, a first dwell then occurs, for 250 ms, before a counter-steer with a negative slope of 720 deg/s begins, until it reaches -150 deg. Then, a second dwell occurs for 3 s, before the steering wheel is returned to its starting position (0 deg) within 2 s. Although typically used for rollover prevention tests, this severe maneuver may also cause spin-out of passenger cars, and is therefore suitable for YSC system testing [40]. The results of this simulation, presented in Figure 4, shows that both controllers manage to stabilize the vehicle. The sideslip angle of the stationary H_∞ is again closer to the desired one, however, the yaw rate response of the GS-H_∞ controller is much better, presenting great tracking and only a minor overshoot.

5.3 Double lane change on low friction road

Using the CarSim's closed-loop driver utility, this test simulates an emergency overtaking maneuver on a slippery road (with $\mu = 0.4$). The driver is driving the vehicle at 120 km/h and tries to follow a predefined path that simulates an emergency overtaking (see Figure 5(d)). This severe maneuver provides an excellent test for the vehicle transient behavior, forces the vehicle and its tire to operate well beyond their linear range. The results of this simulation, presented in Figure 5, show that in this maneuver the stationary H_∞ controller is no longer able to prevent the vehicle spin-out. The inaccurate model underlying its design, caused the motors to saturate and the vehicle to develop large yaw rate and sideslip angle, which as a result departed from its designated path. The GS-H_∞ controller, however, has

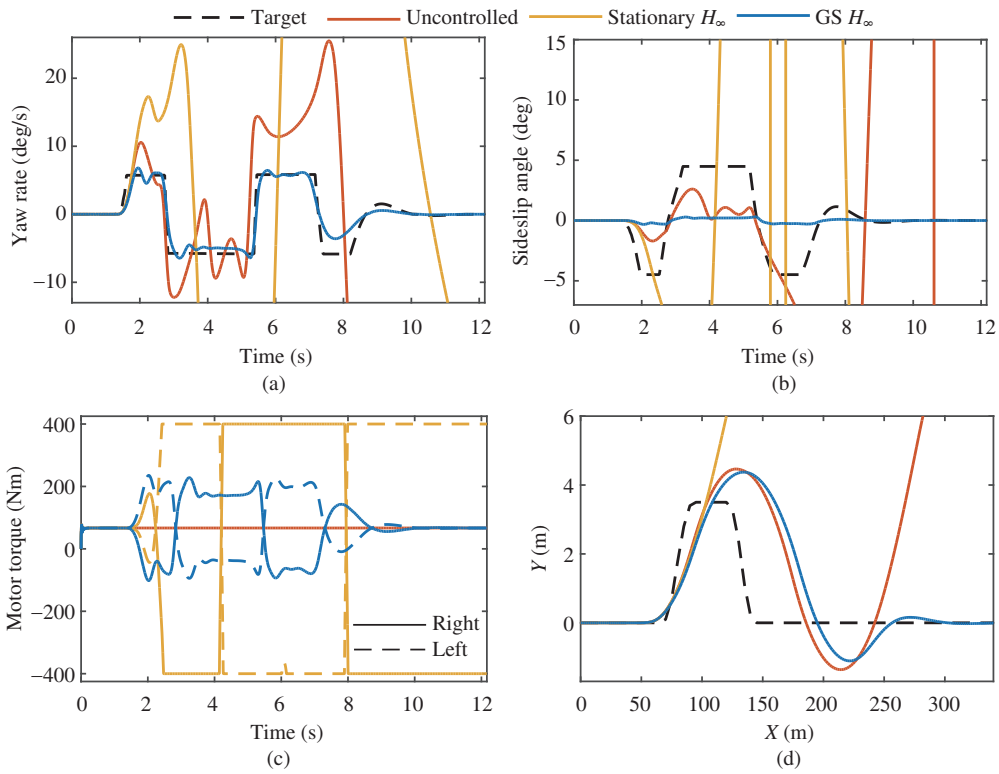

Figure 5 (Color online) Simulation results of double lane change test for gain-scheduled H_∞ controlled, stationary H_∞ controlled and uncontrolled vehicle. (a) Yaw rate; (b) sideslip angle; (c) motor torques; (d) trajectory.

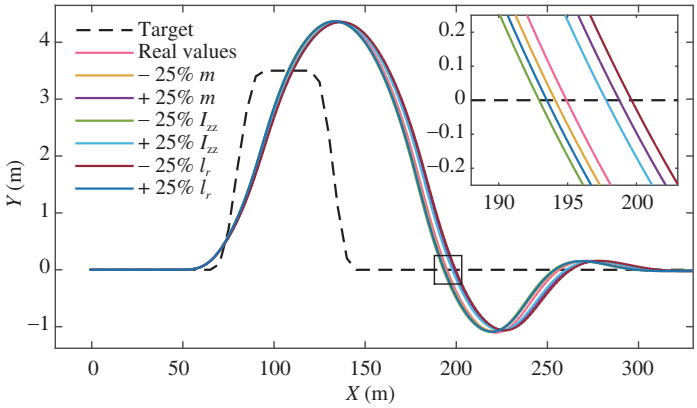

Figure 6 (Color online) Trajectory of a vehicle during double lane change maneuver, controlled by GS-H_∞ controller with parameter errors.

managed to keep the sideslip angle small and accurately tracks the desired yaw rate, despite this extreme maneuver.

5.4 Robustness to model errors

In order to evaluate the robustness of the proposed GS-H_∞ controller to model inaccuracy, deliberate errors were inserted to the vehicle parameters. In this case, errors of 25% in the mass, yaw moment of inertia and center of gravity location, were tested. These errors can simulate a situation of exceptional or uneven loading of the vehicle. The robustness test was performed using the double lane change maneuver, since it is the most severe and challenging maneuver being simulated in this study. The results are presented in Figure 6. It is clearly seen that the model errors' effect on the performance of the controller is negligible. That is to say, the controller is robust to model errors. This robustness can

be attributed to the gain-scheduling approach used here, as well as to the chosen estimation method of the cornering stiffness. We notice that the stiffnesses are calculated such that they satisfy the relations dictated by the 2DOF vehicle model equations of motion at each instant. For this reason, any deviation of model parameters is corrected by an appropriate deviation of the cornering stiffnesses, thus softens the influence of the error.

6 Conclusion

A novel nonlinear yaw stability controller was proposed, using the gain-scheduling and H_∞ techniques. The controller is based on an 2DOF LPV model of the vehicle, which accounts for the variation of the longitudinal velocity as well as variation of the tires' cornering stiffness. Simulations carried out using the CarSim software showed the effectiveness of the controller in various scenarios, providing excellent yaw rate tracking, reduced oscillations and small sideslip angle values. When compared to a stationary H_∞ controller, the GS-H_∞ controller proved to be superior; that was especially noticeable in the double lane change maneuver. The relatively high accuracy of the LPV model allowed the GS-H_∞ to present great performance and prevent actuators saturation even in extreme conditions. Robustness test also showed that the proposed GS-H_∞ controller is robust to model errors. The use of LPV framework allows a stability proved controller, which is not dependent on a priori knowledge of the driving conditions and provides excellent performance, as was seen in all test scenarios.

References

1 Sawase K, Ushiroda Y. Improvement of vehicle dynamics by right-and-left torque vectoring system in various drivetrains. Mitsubishi Motors Tech Rev, 2008, 20: 14–20
2 de Novellis L, Sorniotti A, Gruber P, et al. Comparison of feedback control techniques for torque-vectoring control of fully electric vehicles. IEEE Trans Veh Technol, 2014, 63: 3612–3623
3 NHTSA. FMVSS No. 126 — electronic stability control systems. 2007. https://one.nhtsa.gov/DOT/NHTSA/Rulemaking/Rules/Associated%20Files/ESC_FRIA_%2003_2007.pdf
4 Rajamani R. Vehicle Dynamics and Control. 2nd ed. Berlin: Springer, 2012
5 Park K, Heo S J, Baek I. Controller design for improving lateral vehicle dynamic stability. JSAE Rev, 2001, 22: 481–486
6 Shino M, Nagai M. Yaw-moment control of electric vehicle for improving handling and stability. JSAE Rev, 2001, 22: 473–480
7 Esmailzadeh E, Goodarzi A, Vossoughi G R. Optimal yaw moment control law for improved vehicle handling. Mechatronics, 2003, 13: 659–675
8 Mirzaei M. A new strategy for minimum usage of external yaw moment in vehicle dynamic control system. Transp Res Part C-Emerg Technol, 2010, 18: 213–224
9 Li L, Jia G, Chen J, et al. A novel vehicle dynamics stability control algorithm based on the hierarchical strategy with constrain of nonlinear tyre forces. Veh Syst Dyn, 2015, 53: 1093–1116
10 Doumiati M, Sename O, Molina J J M, et al. Gain-scheduled LPV/H_∞ controller based on direct yaw moment and active steering for vehicle handling improvements. In: Proceedings of the 49th IEEE Conference on Decision and Control, Atlanta, 2010
11 Li J W, Yang H F. The research of double-driven electric vehicle stability control system. In: Proceedings of International Conference on Measuring Technology and Mechatronics Automation, Zhangjiajie, 2009
12 Zhang H T, Zhang J Z. Yaw torque control of electric vehicle stability. In: Proceedings of the 6th International Conference on Information and Automation for Sustainability, Beijing, 2012
13 Delprat S, de Loza A F. High order sliding mode control for hybrid vehicle stability. Int J Syst Sci, 2014, 45: 1202–1212
14 Zhou H L, Liu Z Y. Vehicle yaw stability-control system design based on sliding mode and backstepping control approach. IEEE Trans Veh Technol, 2010, 59: 3674–3678
15 Fu C, Hoseinnezhad R, Hadiashar A B, et al. Direct yaw moment control for electric and hybrid vehicles with independent motors. Int J Veh Des, 2015, 69: 1–4
16 Li F, Wang J, Liu Z. Motor torque based vehicle stability control for four-wheel-drive electric vehicle. In: Proceedings of IEEE Vehicle Power and Propulsion Conference, Dearborn, 2009
17 Brahim G, Abdelkader C, Abdellah L, et al. Adaptive fuzzy PI of double wheeled electric vehicle drive controlled by direct torque control. Leonardo Electron J Pract Technol, 2010, 17: 27–46
18 Barbarisi O, Palmieri G, Scala S, et al. LTV-MPC for yaw rate control and side slip control with dynamically constrained differential braking. Eur J Control, 2009, 15: 468–479

19 Siampis E, Velenis E, Longo S. Rear wheel torque vectoring model predictive control with velocity regulation for electric vehicles. Veh Syst Dyn, 2015, 53: 1555–1579

20 Shamma J S. Analysis and design of gain scheduled control systems. Dissertation for Ph.D. Degree. Cambridge: Massachusetts Institute of Technology, 1988

21 Xiong L, Yu Z, Wang Y, et al. Vehicle dynamics control of four in-wheel motor drive electric vehicle using gain scheduling based on tyre cornering stiffness estimation. Veh Syst Dyn, 2012, 50: 831–846

22 Siampis E, Massaro M, Velenis E. Electric rear axle torque vectoring for combined yaw stability and velocity control near the limit of handling. In: Proceedings of the 52nd IEEE Conference on Decision and Control, Florence, 2013

23 Baslamisli S, Köse E, Anlaş G. Gain-scheduled integrated active steering and differential control for vehicle handling improvement. Veh Syst Dyn, 2009, 47: 99–119

24 Jin X J, Yin G, Chen N. Gain-scheduled robust control for lateral stability of four-wheel-independent-drive electric vehicles via linear parameter-varying technique. Mechatronics, 2015, 30: 286–296

25 Zhang H, Zhang X J, Wang J M. Robust gain-scheduling energy-to-peak control of vehicle lateral dynamics stabilisation. Veh Syst Dyn, 2014, 52: 309–340

26 Zhang H, Wang J M. Vehicle lateral dynamics control through AFS/DYC and robust gain-scheduling approach. IEEE Trans Veh Technol, 2016, 65: 489–494

27 Kaiser G, Liu Q, Hoffmann C, et al. Torque vectoring for an electric vehicle using an LPV drive controller and a torque and slip limiter. In: Proceedings of the 51st IEEE Conference on Decision and Control (CDC), Maui, 2012

28 Yin G D, Chen Q, Qadeer A, et al. Yaw stability of four-wheel-drive electric vehicle based on multi-model predictive control. In: Proceedings of the 34th Chinese Control Conference (CCC), Hangzhou, 2015

29 Green M, Limebeer D J N. Linear Robust Control. Upper Saddle River: Prentice-Hall, 1995

30 Gillespie T D. Fundamentals of Vehicle Dynamics. New York: Society of Automotive Engineers, 1992

31 Milliken W F, Milliken D L. Race Car Vehicle Dynamics. New York: SAE International, 1995

32 Jazar R N. Vehicle Dynamics: Theory and Application. Berlin: Springer, 2009

33 Pacejka H B. Tyre and Vehicle Dynamics. 2nd ed. Oxford: Butterworth-Heinemann, 2006

34 Sierra C, Tseng E, Jain A, et al. Cornering stiffness estimation based on vehicle lateral dynamics. Veh Syst Dyn, 2006, 44: 24–38

35 Mohammadpour J, Scherer C. Control of Linear Parameter Varying Systems with Applications. Berlin: Springer, 2012

36 Apkarian P, Gahinet P, Becker G. Self-scheduled H^{∞} control of linear parameter-varying systems: a design example. Automatica, 1995, 31: 1251–1261

37 Briat C. Linear parameter-varying and time-delay systems: analysis, observation, filtering & control. In: Advances in Delays and Dynamics. Berlin: Springer, 2015

38 Wu F K, Yeh T J, Huang C F. Motor control and torque coordination of an electric vehicle actuated by two in-wheel motors. Mechatronics, 2013, 23: 46–60

39 Boyd P L. NHTSA's NCAP rollover resistance rating system. 2005. http://pdfs.semanticscholar.org/e386/b799159bc90ce986ce680ba89db02b5fcf90.pdf

40 Limroth J. Real-time vehicle parameter estimation and adaptive stability control. Dissertation for Ph.D. Degree. Clemson: Clemson University, 2009